Detecting Gaps in Protoplanetary Disks with MIDI at the VLTI

Sebastian Wolf[1], Thomas Henning[2], and Gennaro D'Angelo[2]

[1] Thüringer Landessternwarte Tautenburg, Sternwarte 5, D–07778 Tautenburg, Germany
[2] Astrophysikalisches Institut und Universitäts-Sternwarte Jena, Schillergässchen 2-3, D–07745 Jena, Germany

Abstract. Numerical simulations show that a Jupiter mass planet is able to dig the gas material along its path. Resulting from this, a density gap is produced within the disk which may represent a very large scale density feature.

Based on these hydrodynamical simulations we investigate the possibility to trace planets in circumstellar disks by means of infrared interferometry. On the basis of three-dimensional self-consistent radiative transfer calculations, images of this system were created which provide the basis for the simulation of the VLTI equipped with MIDI. We find that MIDI can be used to distinguish between different disk models – disks with or without an embedded planet – on the basis of the observed visibilities.

1 Introduction

Based on studies of the evolution of protoplanets in protostellar disks, it has been established that - depending on the hydrodynamic properties of the planet and the disk - giant protoplanets may open a gap and cause spiral density waves in the disk (see, e.g., Kley 1999, 2001). The gap may extend up to several AU in width. Thus, the question arises if one can find such a gap as an indicator for the presence of a protoplanet with present-day or near-future techniques. In order to study this possibility, we used hydrodynamical simulations of a protostellar disk with an embedded planet (§ 2) to compute the expected brightness distributions, using a 3D radiative transfer (RT) code. Based on subsequent calculations of the visibility of this source we show that interferometers such as the VLTI of the European Southern Observatory equipped with the MIDI (Midinfrared Interferometric Instrument) in the mid-infrared provides the necessary basis to detect gaps in circumstellar disks (§ 3).

2 Hydrodynamical Simulations

The presence of a massive body within a circumstellar disk affects its structure very rapidly. Already after 10 planet's revolutions the gap has developed along with the spiral patterns, as displayed in the left panel of Fig. 1. The other two panels of this Figure show the evolution of the gap and the spirals and how they appear at later times.

This simulation has been performed using a smaller radial extent ([2, 13] AU) to increase the resolution of both the gap and the spiral density waves. However, the density waves propagate beyond 13 AU. Figure 1 also indicates that along the orbit of the planet the gap is not dug everywhere at the same rate. After 10 orbits – while the density has already dropped of the 60% in the vicinity of the planet – two bumps still exist around the Lagrangian points L_4 and L_5, where the density has reduced to only 30%. However, also this material is removed later on during the evolution of the system (see Fig. 2).

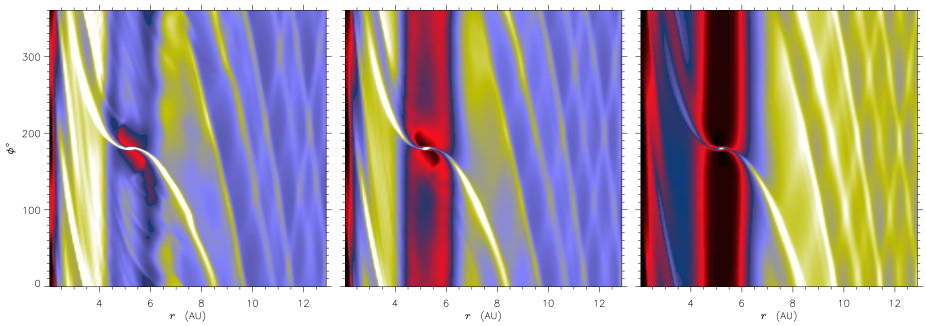

Fig. 1. Three snapshots reproducing the surface density distribution after 10 (left), 50 (center) and 300 (right) orbital periods. At the location of the planet $r_{\rm p}$, the resolution of the grid is such that $\varDelta r = r_{\rm p}\,\varDelta\phi = 0.078$ AU.

The azimuthally averaged depth of the gap settles to a constant value around 100 orbital periods. Anyway, the disk inside the orbit of the planet keeps on depleting because material is allowed to flow out of the computational domain through the inner radial border. This choice is intended to simulate the drifting of the gas towards the central star.

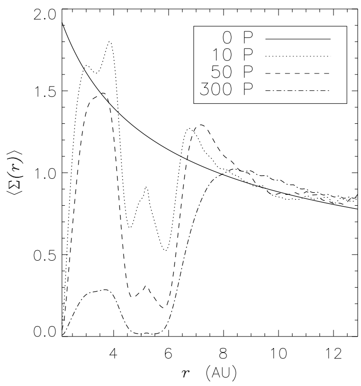

Fig. 2. Evolution of the azimuthally averaged surface density distribution. The peaks within the gap are due to the material lingering around the two triangular Lagrangian points located on the orbit of the planet, 60° away from it. This happens because these points represent positions of stable equilibrium for the restricted three-body problem. At 50 orbital periods they nearly vanish.

The formation of the gap basically depends on the balance of two competing processes. On one hand there are the gravitational torques, exerted by the planet, which reduce the angular momentum of the inside-orbit material (at $r \lesssim r_{\mathrm{p}}$) and increase that of the outside-orbit one (at $r \gtrsim r_{\mathrm{p}}$). As a result, the gas is cleared out along the planet's path. On the other hand the viscous torques work to smooth the surface density and thus they oppose to the former process.

As the mass of the perturber reduces, the efficency of the gravitational torques reduce too, hence the gap becomes shallower. This can be clearly seen in Fig. 3, where both the surface density and its azimuthal mean are compared for models with planets of different masses.

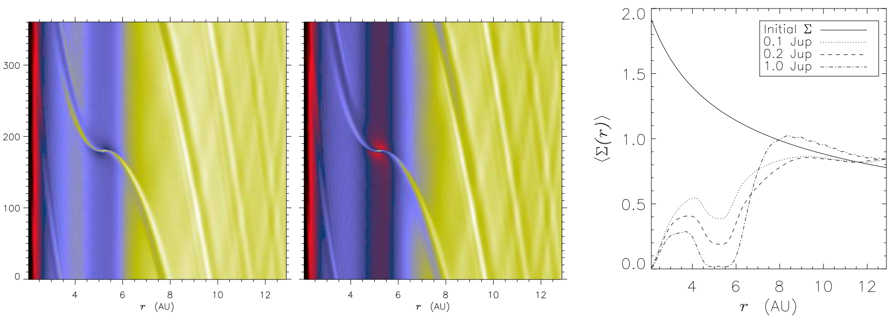

Fig. 3. Gap from models with planets of different masses: 0.1 (left) and 0.5 (center) Jupiter masses. The averaged surface density $\langle \Sigma(r) \rangle$ reported in the right panel, clearly shows how viscous torques fill the gap as the planet's mass reduces.

3 Simulations of observations with MIDI

In the following we consider a protostellar disk with a density profile resulting from hydrodynamical simulations. The disk is assumed to be flat and non-self-gravitating. The mutual gravitational interaction between the planet and the central star, and the gravitational torques of the disk acting on the planet and the central star are included. Drifting of disk material onto the central star is prevented during these simulations. The three-dimensional density structure is Gaussian in the vertical direction where for the scale height H(r) we assume a constant ration H/r=0.05. The undisturbed (no gap) surface density distribution was given by $\Sigma \propto r^{-1/2}$.

The mass of the star is assumed to be 1 $\mathrm{M_{sun}}$, the mass of the planet is 1 Jupiter mass, and the mass of the disk is 0.05 $\mathrm{M_{sun}}$. For the dust-to-gas mass ratio we take the classical value of 1:100. The diameter of the disk is 104 AU which is comparable to the size of the disk seen in silhouette against the Orion Nebula (McCaughrean & O'Dell 1996). The planet is located at a distance of 5.2 AU from the star. The structure of the spirals and the gap reaches an equilibrium after about 150 orbits. The specifics of the models and the results, in particular the width and internal structure of the gap, are described in detail in Kley (1999) and Kley et al. (2001).

Based on this density distribution we simulated the dust continuum emission of the dust. The RT has been performed with a 3D continuum code which is based on the Monte Carlo method. The RT is simulated self-consistently taking into account both the initial temperature of the dust due to viscous heating and the additional energy input of the central star. The dust density and temperature structure are defined on a grid which is chosen to be identical with that of the hydrodynamical simulations. Thus, any additional discretization error resulting from the "transfer" of the density/temperature structure to the RT code is avoided. For further information concerning the RT code, we refer to Wolf et al. (1999) and Wolf & Henning (2000).

In addition to the results from the hydrodynamical simulations, we introduce the following RT parameters: spherical dust grains consisting of "astronomical" silicates (optical data from Draine & Lee 1984, radius $0.12\,\mu$m); star: effective temperature $T_{\rm eff} = 5500\,$K, luminosity $L = 1\,{\rm L}_{\rm sun}$; wavelength range for the simulation of the radiative transfer: $0.03 \ldots 2000\,\mu$m.

As the first step towards visibility calculations we simulated images of the disk in the near-infrared...submillimetre wavelength range. Due to the huge intensity peak caused by warm/hot dust located very close to the star (1...2 AU), the outer regions of the disk remain dark at near/mid-infrared wavelengths. The gap located at 5 AU can be hardly seen. In contrast to this, in the submillimetre/millimetre wavelength range the brightness distribution is much smoother. This can be explained by the behaviour of the Planck function $B_\lambda(T)$. The ratio $B_\lambda(T_1)/B_\lambda(T_2)$ $(T_1 > T_2)$ strongly decreases with increasing wavelength. Thus, the flux ratio and the brightness contrast between regions characterized by different dust temperatures (T_1 and T_2) decreases with increasing wavelength λ.

In Figure 4 visibility curves at λ=10 μm for different inclinations of the disk are shown (with/without gap). The goal of these simulations is to check whether MIDI at the VLTI can be used to detect gaps. The visibilitiy V has been calculated based on the spatial intensity distribution $I(x, y)$ derived beforehand:

$$\Gamma(u,v) = V e^{i\Phi_{\rm V}} = \int\int I(x,y) \exp\left[-2\pi i(ux+vy)\right] dx\, dy\,. \tag{1}$$

Here, $\Phi_{\rm V}$ is the phase function and $\Gamma(u, v)$ the complex visibility of the radiative source (see Pearson & Readhead 1984 and Shao & Colavita 1992 for details).

In the case of a disk with a gap, the visibility shows a steeper decrease. This decrease strongly depends on the inclination of the disk i and the relative orientation between the direction of the baseline between the two telescopes and the major axis of the ellipse resulting from the projection of the disk onto the plane of the sky. The differences in the visibility profiles at a fixed inclination i result from the different density distributions in the inner, warm region of the

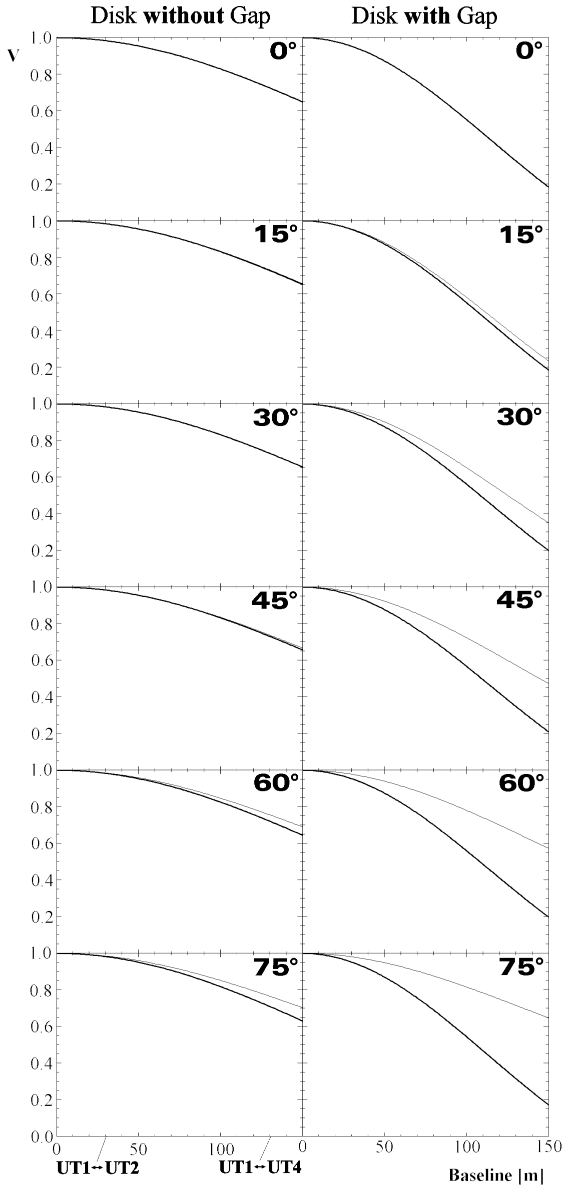

Fig. 4. Normalized visibilities at λ=10 μm for disks with an inclination of $i = 0^{\circ}$ (face-on), 15°, 30°, 45°, 60°, and 75° (right column; assumed distance: 140 pc). For comparison the same profiles in the u-v plane but for a disk without a gap (but with the same mass and inclinations) are also given (left column). The visibilities marked by the thick and the thin line are oriented perpendicular to each other in the u-v plane (parallel to the major/minor axis of the ellipse resulting from the projection of the disk onto the plane of the sky). We would like to mention that the exact shape of the visibility depends on the details of the hydrodynamical simulations.

disk (within a radius of 3 AU around the star) caused by the planet's motion and not from the gap. Furthermore, in Figure 4 the distances between the telescope UT1 and UT2 resp. UT1 and UT4 of the VLTI are indicated. Taking into account uncertainties of "real" measurements (e.g. with MIDI - the mid-infrared interferometric instrument for the VLTI), a distinction between different disk models (with/without gap) based on significant differences between the visibility profiles is possible only by a beam combination of the most distant telescopes of the VLTI.

4 Conclusions

We investigated the influence of a massive body – such as a protoplanet – on the density structure in a protoplanetary disk. We showed that the planet – depending on its mass – clears out the material on its path and thus opens a gap in the disk. Although the spatial extend of the gap is much larger than the planet itself, the gap is too small to be mapped using recent observational techniques (assuming the disk to be located in nearby star-forming systems).

However, based on the hydrodynamical simulations and subsequent 3D RT simulations we derived the visibilities at $10\,\mu$m as a function of the baseline assuming a two-beam interferometer. It turned out that MIDI at the VLTI can be used to distinguish between different disk models on the basis of the observed visibilities. However, the longest possible baseline is required.

5 Acknowledgments

We wish to thank W. Kley for providing his results from hydrodynamical simulations discussed in § 3.

References

1. Draine, B.T., Lee, H.M., 1984, ApJ, 285, 89
2. Kley, W., 1999, MNRAS, 303, 696
3. Kley, W., D'Angelo, G., Henning, Th., 2001, ApJ, 547, 457
4. McCaughrean, M.J., O'Dell, C.R., 1996, ApJ, 111, 1977
5. Pearson, T.J., Readhead A.C.S, 1984, ARA&A 22, 97
6. Shao, M., Colavita M.M., 1992, ARA&A 30, 457
7. Wolf, S., Henning, Th., 2000, Comp. Phys. Comm. 132, 166
8. Wolf, S., Henning, Th., Stecklum, B., 1999, A&A, 349, 839